Energy optimal design of servo-actuated systems: a concurrent approach based on scaling rules

Paolo Boscariol*[1] and Dario Richiedei[1]

[1]Dipartimento di Tecnica e Gestione dei sistemi industriali, Università degli Studi di Padova

Abstract

This paper addresses the issue of reducing the energy consumption of servo-actuated systems by means of the optimal selection of the electric motor and of the gearbox from catalogs of commercially available components. This idea overcomes a lack of literature: on the one hand, the energy efficiency of these systems is usually tackled through the improvement of the efficiency of each individual component rather than on focusing on a global efficiency goal; on the other one, the methods to select these components neglect the specific issue of energy consumption, being usually focused on cost reduction or minimum motor sizing. The aim of this paper is to propose a model-based design approach for the energy-optimal concurrent selection of motor, coupling and gearbox in servo-actuated systems. The method is based on the use of scaling rules, which are developed to condensate all the relevant characteristics of the system into just two parameters: the gearbox transmission ratio and the motor continuous torque at stall. Scaling rules summarize and reveal the complex relations between the system parameters and energy consumption, and hence are incorporated into the analytic formulation of the overall energy consumption. The use of these metamodels, that can be easily obtained from data provided in datasheets, allows casting the design problem as a constrained optimization problem with just two design variables. The outlined procedure is completely automatic and does not require any design iteration. The results, evaluated for two application examples, demonstrate the relevant energy savings provided by the proposed method.

Highlights:

- Energy-optimal design procedure for servo-actuated mechatronic systems
- Use of scaling rules to represent the relevant components from catalogue data

*Corresponding author: paolo.boscariol@unipd.it

This is a pre-print of the article: P. Boscariol, D. Richiedei
Energy optimal design of servo-actuated systems: a concurrent approach based on scaling rules
Renewable and Sustainable Energy Reviews, Volume 156, March 2022, 111923
https://doi.org/10.1016/j.rser.2021.111923

- Scaling rules do not affect the accuracy of the energy estimation model
- A significant energy reduction is achieved
- The method is appealing for scientists and industry practitioners

Keywords: energy efficiency; brushless motors; servo motors; mechatronics; servo motor design; gearbox efficiency; equipment selection; energy optimal design;

1 Introduction

Servo-controlled electric motors, together with the related power electronic devices and mechanical transmissions, are key components of mechatronic systems, automatic machines and robots and are ever more adopted in modern industry. Several studies show that the electric energy absorbed by the electric motors accounts for up to the 70% of the total energy consumed in the industrial sector [1, 2]. Therefore, a great effort by motor manufacturers and a great attention by academic studies have been devoted to enhance the efficiency of of electric motors and of the auxiliary electronic and mechanical components. This trend is also boosted by government policies and guidelines supporting the transition to a 'low-carbon' industry. The literature reviews in [1, 3, 4], and the references therein, discuss the most important technological challenges that should be faced for developing the so-called 'super premium efficient motors', that mainly include new design paradigms and new materials. Recently, attention has been focused on the optimal design of the mechanism to be driven by the motors, by exploiting lightweight design [5] or springs to accumulate energy [6] or to exploit resonances in the presence of harmonic motion [7]. Optimal motion planning has been shown to allow for meaningful energy saving as well [8], without requiring any physical modification to the servo-actuated system. In contrast, the effect of the proper sizing of the electric motor and of the mechanical transmission is often underrated, although the problem of energy increases due to a wrong motor sizing has been sometimes recognized in the literature [3, 9]. Some studies have addressed the relation between motor oversizing and energy consumption for three-phase induction motors [10]. The problem treatment is different and the difficulties in choosing energy-optimal motors and mechanical transmissions are even greater in the case of servo-controlled axis where variable-speed motors (such as brushless or DC motors) are used to track time-varying motion laws with imposed speed and acceleration profiles. Indeed, besides the motor size, the transmission ratio (such as the gear ration in the case of speed reducers) has a considerable impact on the overall energy consumption. Despite this relevance, the issue of energy-optimal component selection has been not comprehensively investigated since different goals are traditionally set in designing these systems.

Traditionally designers choose a motor-reducer set by first choosing the speed reducer from a catalog, according to the estimated characteristics of the load, and then by choosing the most suitable motor through a sequential approach.

This is a pre-print of the article: P. Boscariol, D. Richiedei
Energy optimal design of servo-actuated systems: a concurrent approach based on scaling rules
Renewable and Sustainable Energy Reviews, Volume 156, March 2022, 111923
https://doi.org/10.1016/j.rser.2021.111923

The selection of the motor and of the transmission ratio is usually aimed at minimizing the motor size and hence, its purchasing cost. This design philosophy is usually suggested in manufacturers' datasheet, such as in [11]. This method is generally supported by simple calculations based on simplified models that just partially represent the system dynamics. A typical approach is, for example, to assume a purely inertial load (with constant moment of inertia), as in [12], where the well-known inertia-matching condition is formulated. Such a condition, that is widely adopted by practitioners and design engineers, is aimed at maximizing load acceleration for a purely inertial load and with ideal gearboxes. This design method is rather inefficient, as it requires frequent trial-and-error iterations starting from the initial choice to reach a feasible design and to converge towards the most suitable solution. Furthermore, there are no guarantees of a complete exploration of all the possible solutions. Additionally, the inertia-matching condition is usually inefficient in term of energy consumption [13]. The assumption of ideal components is also adopted in more recent papers. For example the paper [14] assumes ideal gearboxes and a very basic description of the motor's speed-torque characteristic curve. The work [15] is also worth of mention: it proposes a method for the simultaneous choice of both gearbox and motor in the case of purely inertial loads and by assuming a simple motor characteristic curve. The extension of this work to a generic load is provided in [16], by assuming again a simplified motor model with a rectangular operative range. Multi-criteria selection methods have been adopted as well to accomplish more elaborate design objectives. The work [17] proposes a method for the choice of the motor and the reducer, starting from information extracted from datasheets, which are used to choose a set of possible candidates for the design. The procedure then eliminates the unsuitable components, leaving the final choice to the designer according to the chosen metric (e.g. size, cost, weight) to be favored. The proposed procedure however does not lead to the definition of an optimal gear ratio, and the effect of the gear ratio on the properties of the transmission is neglected. The work [18] focuses on the optimal selection of the six motors of an industrial robot. The result is an optimal design, obtained through a multi-criteria optimization aimed at minimizing the energy consumption, tracking error and motor weight. Given the complexity of the modeling and the large number of constraints, the optimal design is achieved by a genetic algorithm. As in other works, the description of the motors operative range is limited to a rectangular shape, and the choice of the reducers is not performed by the algorithm. Additionally, a simplified model of the energy consumption is assumed.

A comprehensive method for the design optimization of a motor-reducer set is developed in [19]. Such a method casts the selection from discrete catalogs as a continuous optimization problem, by interpolating the parameters made available by the motor catalogue on the basis of a so-called 'size index', and by interpolating the reducers parameters on the basis of the gear ratio. Interpolation is therefore used to transform a discrete set of components into a continuous one, easing the numerical optimization problem that drives the design.

This is a pre-print of the article: P. Boscariol, D. Richiedei
Energy optimal design of servo-actuated systems: a concurrent approach based on scaling rules
Renewable and Sustainable Energy Reviews, Volume 156, March 2022, 111923
https://doi.org/10.1016/j.rser.2021.111923

The idea of using continuous functions to represent catalogues in the design of a servo-controlled axis is also proposed by Richiedei in [20]. Compared to [19], a more comprehensive approach is proposed, by exploiting the concept of scaling rules introduced in [21], instead of the simpler interpolations adopted in [19]. The use of scaling rules allows representing the scaling of the gearbox and motor properties in a complete way, by means of two driving parameters: the gear ratio and the continuous torque at stall of the motor. This formulation leads to the concurrent optimal design of the speed reducer, the motor and the mechanical coupling, to minimize the RMS (Root Mean Square) motor torque, and therefore the motor size and its purchasing cost.

The idea proposed in [20] is revisited and extended in this work with the goal of finding the optimal combination of motor and gearbox to reduce the energy consumption. Several scaling rules are proposed and validated with the experimental data provided by by manufacturers in datasheet and adopted in a comprehensive model that estimates the electric energy required to perform a cyclic task, while accounting for losses in the whole system. A novel method to perform energy optimal design of the servo-actuated system is then formulated. While the 'minimum motor sizing' in [20] is the 'cheapest initial cost' solution, the 'energy-optimal sizing' proposed here minimizes the energy cost and impact, leading to a cheaper operation in the long run. Two examples on the use of this novel design approach are proposed in the paper, referring to a constant and to a variable inertia load.

2 System modeling: mechanical model

The system under investigation is composed by cascading an electric motor, a coupling, a gearbox and a rotating load, as shown in figure 1. Such a model can represent several automatic machines and mechatronic systems, and therefore can be applied to various industrial fields.

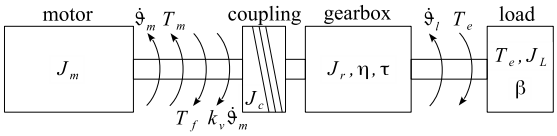

Figure 1: Model of the system

The speed of the motor shaft is $\dot{\vartheta}_m$, while the speed of the load shaft is $\dot{\vartheta}_l$. The torque provided by the motor is referred to as T_m, while the external torque applied to the load shaft is T_e. Friction forces on the motor side are included too. The inertial properties of the system are represented by the moments of inertia J_m, J_c, J_r and J_l, which are the moment of inertia of the motor, of the coupling, of the gearbox and of the load, respectively. The gearbox moment of inertia is the reflected moment of inertia as measured on its input side, according to the common convention.

This is a pre-print of the article: P. Boscariol, D. Richiedei
Energy optimal design of servo-actuated systems: a concurrent approach based on scaling rules
Renewable and Sustainable Energy Reviews, Volume 156, March 2022, 111923
https://doi.org/10.1016/j.rser.2021.111923

The speed reduction implemented by the gearbox is represented by the transmission ratio τ:

$$\tau = \frac{\dot{\vartheta}_l}{\dot{\vartheta}_m} = \frac{1}{i} \tag{1}$$

Equation (1) also shows that the transmission ratio τ is the reciprocal of the gear ratio i. The gearbox efficiency is represented by the generalized efficiency $\eta(t)$, which is in practice hardly described by a constant value, due to the uneven power transmission shown according to the power flow direction. Direct efficiency η_d represents the efficiency of the gearbox when the power flows from the motor to the load, while reverse efficiency η_r accounts for the opposite power flow direction. This asymmetry is represented by the the discontinuous function:

$$\eta(t) = \begin{cases} \eta_d & \text{if} \quad \left(T_e + J_l\ddot{\vartheta}_l + k_f\dot{\vartheta}_l\right)\dot{\vartheta}_l > 0 \quad \text{(direct power flow)} \\ \dfrac{1}{\eta_r} & \text{if} \quad \left(T_e + J_l\ddot{\vartheta}_l + k_f\dot{\vartheta}_l\right)\dot{\vartheta}_l < 0 \quad \text{(reverse power flow)} \end{cases} \tag{2}$$

Equation (2) shows how the value of η is parametrized by the sign of the power flow to the load: when it is negative, the load is providing positive mechanical power to the system and the motor acts as a brake. The torque contribution that appear in eq.(2) can be condensed in a single term, usually denoted T_2:

$$T_2(t) = T_e(t) + J_l\ddot{\vartheta}_l(t) + k_f\dot{\vartheta}_l(t) \tag{3}$$

In this case T_2 is composed by an inertial term, a viscous friction term (modeled through the load-side viscous friction coefficient k_f), and the external torque $T_e(t)$, that can be either constant or time-varying. The profile of $T_2(t)$ can be computed from the load speed and acceleration profiles. More generally, T_2 can be any arbitrary load torque, that might be related, for example, to the case of a variable inertia load. A common technique to model a variable inertia load is to use the concept of reflected inertia, so that the torque required to actuate a single degree-of-freedom multibody system can be computed by using the Lagrangian model:

$$T_2(t) = J_l^{eq}(\vartheta_l)\ddot{\vartheta}_l(t) + \frac{1}{2}\frac{dJ_l^{eq}}{d\vartheta_l}\dot{\vartheta}_l^2(t) + T_e(t) \tag{4}$$

The reflected inertia measured on the load side, $J_l^{eq}(\vartheta_l)$, can be computed as the sum of all the inertias multiplied by the square value of the sensitivity coefficients that relate the displacement of the i-th mass and the i-th moment of inertia to the displacement ϑ_l:

$$J_l^{eq}(\vartheta_l) = \sum_i m_i \left(\frac{\partial p_i}{\partial \vartheta_l}\right)^2 + J_i \left(\frac{\partial \varphi_i}{\partial \vartheta_l}\right)^2 \tag{5}$$

This is a pre-print of the article: P. Boscariol, D. Richiedei
Energy optimal design of servo-actuated systems: a concurrent approach based on scaling rules
Renewable and Sustainable Energy Reviews, Volume 156, March 2022, 111923
https://doi.org/10.1016/j.rser.2021.111923

where the sensitivity coefficient $\frac{\partial p_i}{\partial \vartheta_l}$ relates the absolute displacement of the center of mass of the i-th body with the angular displacement ϑ_l, while $\frac{\partial \varphi_i}{\partial \vartheta_l}$ relates the angular displacement of the i-th body with the displacement ϑ_l. Each J_i is the barycentric moment of inertia of the i-th body. The reflected torque $T_e(t)$ can be computed by reflecting all the external forces, enumerated as F_j, through the sensitivity coefficients $\frac{\partial s_j}{\partial \vartheta_l}$ that relate each Lagrangian displacement s_j with the angular displacement of ϑ_l as:

$$T_e(t) = \sum_j F_j \frac{\partial s_j}{\partial \vartheta_l} \tag{6}$$

3 Motor power consumption estimation

The aim of this section is to define an analytic expression of the energy consumption of the motor-coupling-gearbox-load: such a formulation will then be used to drive the system design optimization. When obvious, explicit time dependency is not shown in the formulas that will follow, to provide an easier to read formulation.

The dynamic model of the servo-actuated system already shown in Fig.1 can be written as a torque balance equation. The motor needs to provide the torque $T_m(t)$ to compensate for its own inertia, as well as for the inertias of the coupling J_c and of the gearbox, J_r. Static and viscous friction torques acting on the motor shaft, represented as T_f and $k_v\dot{\vartheta}_m(t)$, respectively, are considered as well. Finally, the reflected valued of the load torque $T_2(t)$ needs to be compensated as well. The motor must therefore provide the following instantaneous torque:

$$T_m = (J_m + J_r + J_c)\frac{\ddot{\theta}_l}{\tau} + k_v\frac{\dot{\theta}_l}{\tau} + T_f + \tau\frac{T_2}{\eta} \tag{7}$$

The electric power flow to the motor can be modeled by an equivalent DC motor, according to the well known Park's direct-quadrature-zero transformation [22], following the procedure used in other works such as [23, 24, 25]. Such a simple model can be used to describe not only DC motors, but also brushless motors, and with some modifications, to single-phase and three-phase induction motors [26].

The voltage drop across the motor windings can be computed as:

$$V(t) = RI(t) + k_b\dot{\vartheta}_m(t) + L\frac{dI(t)}{dt} \tag{8}$$

in which R and L are the equivalent resistance and the inductance, respectively, of the motor windings and k_b is the motor back-emf constant. Motor current $I(t)$ is proportional to the exerted torque through the torque constant k_t:

This is a pre-print of the article: P. Boscariol, D. Richiedei
Energy optimal design of servo-actuated systems: a concurrent approach based on scaling rules
Renewable and Sustainable Energy Reviews, Volume 156, March 2022, 111923
https://doi.org/10.1016/j.rser.2021.111923

$$T_m(t) = k_t I(t) \tag{9}$$

The electric power drawn by the electric motor can be computed as the voltage-current product:

$$P_m(t) = V(t)I(t) \tag{10}$$

The time integral of the electric power, defined over the time frame $[0, T]$, defines the motor energy absorbed during a working cycle lasting T. Using equations (8-10), the latter can be written as:

$$E_m = \int_0^T VIdt = \int_0^T RI^2dt + \int_0^T k_b\dot{\theta}_m Idt = \frac{R}{k_t^2}\int_0^T T_m^2 dt + \frac{k_b}{k_t}\int_0^T \dot{\theta}_m T_m dt \tag{11}$$

Equation (11) does not include the inductance term L, since it does not affect the energy dissipation [8]. The first of the two terms in eq.(11) is the energy due to Joule losses $E_{m,joule}$, while the second one is the energy consumption due to mechanical losses $E_{m,mech}$:

$$E_m = E_{m,joule} + E_{m,mech} \tag{12}$$

$E_{m,joule}$ is computed through the square value of the RMS motor torque as:

$$E_{m,joule} = \frac{R}{k_t^2}\int_0^T T_m^2 dt = T\frac{R}{k_t^2}(T_{m,RMS})^2 \tag{13}$$

The square value of the motor RMS torque can be computed using eq.(7), in which the inertia contributions at the motor shaft are collected into the total equivalent inertia, J_1, as $J_1 = J_m + J_r + J_c$:

$$T_{m,RMS}^2 = \left(J_1\frac{\ddot{\theta}_l}{\tau} + \tau\frac{T_2}{\eta} + k_v\frac{\dot{\theta}_l}{\tau} + T_f\right)_{RMS}^2 \tag{14}$$

The term T_m is, according to eq.(14), written as the sum of four terms, and therefore its square RMS value can be written as a combination of RMS values and mean values:

$$\begin{aligned} T_{m,RMS}^2 = &\left(\frac{J_1\ddot{\theta}_l}{\tau}\right)_{RMS}^2 + \left(\tau\frac{T_2}{\eta}\right)_{RMS}^2 + \left(k_v\frac{\dot{\theta}_l}{\tau}\right)_{RMS}^2 + T_{f\,RMS}^2 \\ &+2\left(\frac{J_1\ddot{\theta}_l T_2}{\eta}\right)_{mean} + 2\left(\frac{J_1 k_v\dot{\theta}_l\ddot{\theta}_l}{\tau^2}\right)_{mean} + 2\left(\frac{J_1\ddot{\theta}_l T_f}{\tau}\right)_{mean} \\ &+2\left(\frac{T_2 k_v\dot{\theta}_l}{\eta}\right)_{mean} + 2\left(\frac{\tau T_2 T_f}{\eta}\right)_{mean} + 2\left(\frac{k_v\dot{\theta}_l T_f}{\tau}\right)_{mean} \end{aligned} \tag{15}$$

This is a pre-print of the article: P. Boscariol, D. Richiedei
Energy optimal design of servo-actuated systems: a concurrent approach based on scaling rules
Renewable and Sustainable Energy Reviews, Volume 156, March 2022, 111923
https://doi.org/10.1016/j.rser.2021.111923

Now, by using eq.(13), the energy dissipated by the motor through Joule losses can be computed as:

$$\begin{aligned} E_{m,joule} = T\frac{R}{k_t^2}\left[\frac{J_1^2}{\tau^2}\left(\ddot{\theta}_{l,RMS}\right)^2 + \tau^2\left(\frac{T_2}{\eta}\right)^2_{RMS} + \frac{k_v^2}{\tau^2}\left(\dot{\theta}_{l,RMS}\right)^2 + T_f^2\right] \\ +T\frac{R}{k_t^2}\left[2J_1\left(\frac{\ddot{\theta}_l T_2}{\eta}\right)_{mean} + 2\frac{J_1 k_v}{\tau^2}\left(\dot{\theta}_l\ddot{\theta}_l\right)_{mean} + 2\frac{J_1 T_f}{\tau}\ddot{\theta}_{l,mean}\right] \\ +T\frac{R}{k_t^2}\left[2k_v\left(\frac{T_2\dot{\theta}_l}{\eta}\right)_{mean} + 2\tau T_f\left(\frac{T_2}{\eta}\right)_{mean} + 2\frac{k_v T_f}{\tau T}h\right] \end{aligned} \tag{16}$$

This expression becomes simpler for a rest-to-rest motion, given that the mean values of both $\dot{\vartheta}_l\ddot{\vartheta}_l$ and $\ddot{\vartheta}_l$ are equal to zero:

$$\int_0^T \dot{\vartheta}_l\ddot{\vartheta}_l dt = 0 \tag{17}$$

$$\int_0^T \ddot{\vartheta}_l dt = 0 \tag{18}$$

For a rest-to-rest motion, therefore, the first term of the energy consumption can be written as:

$$\begin{aligned} E_{m,joule} = T\frac{R}{k_t^2}\left[\frac{J_1^2}{\tau^2}\left(\ddot{\theta}_{l,RMS}\right)^2 + \tau^2\left(\frac{T_2}{\eta}\right)^2_{RMS} + \frac{k_v^2}{\tau^2}\left(\dot{\theta}_{l,RMS}\right)^2 + T_f^2\right] \\ +T\frac{R}{k_t^2}2J_1\left(\frac{\ddot{\theta}_l T_2}{\eta}\right)_{mean} \\ +T\frac{R}{k_t^2}\left[2k_v\left(\frac{T_2\dot{\theta}_l}{\eta}\right)_{mean} + 2\tau T_f\left(\frac{T_2}{\eta}\right)_{mean} + 2\frac{k_v T_f}{\tau T}h\right] \end{aligned} \tag{19}$$

The energy consumption due to mechanical losses takes a simpler form:

$$E_{m,mech} = \frac{k_b}{k_t}\int_0^T \dot{\theta}_m T_m dt = \frac{k_b}{k_t}\frac{1}{\tau}\int_0^T \dot{\theta}_l T_m dt \tag{20}$$

Again, using eq.(7), the mechanical energy loss is:

$$E_{m,mech} = \frac{k_b}{k_t}\frac{1}{\tau}\left[J_1\int_0^T \frac{\dot{\theta}_l\ddot{\theta}_l}{\tau}dt + \tau\int_0^T \frac{T_2}{\eta}\dot{\theta}_l dt + \frac{k_v}{\tau}\int_0^T {\dot{\theta}_l}^2 dt + T_f\int_0^T \dot{\theta}_l dt\right] \tag{21}$$

The term $\int \dot{\vartheta}_l\ddot{\vartheta}_l dt$ is equal to zero for a rest-to-rest motion. Eq.(21) can be therefore rewritten by recognizing the mean value of $T_2\dot{\vartheta}_l/\eta$, the square

This is a pre-print of the article: P. Boscariol, D. Richiedei
Energy optimal design of servo-actuated systems: a concurrent approach based on scaling rules
Renewable and Sustainable Energy Reviews, Volume 156, March 2022, 111923
https://doi.org/10.1016/j.rser.2021.111923

RMS value of the load speed, and the constant term proportional to the overall displacement of the load, h, as:

$$E_{m,mech} = T\frac{k_b}{k_t}\left(\frac{T_2\dot{\theta}_l}{\eta}\right)_{mean} + T\frac{k_b}{k_t}\frac{k_v}{\tau^2}\dot{\theta}^2_{l,RMS} + \frac{k_b}{k_t}\frac{T_f}{\tau}h \tag{22}$$

The model of the motor energy consumption can be further refined to take into account the effects of the motor driver as well, by introducing its efficiency, thus providing a more accurate estimation of the actual energy drawn from the electric distribution system, as:

$$E_{tot} = \eta_{driver}\left(E_{m,joule} + E_{m,mech}\right) \tag{23}$$

In principle, eq.(23) could be adopted to find the optimal transmission ratio that minimizes the energy consumption by considering E_{tot} as just a function of the parameter τ, whose optimal value can be found as the solution to the equation:

$$\begin{aligned} RT\left(\frac{T_2}{\eta}\right)^2_{RMS}\tau^4 + 2TRT_f\left(\frac{T_2}{\eta}\right)_{mean}\tau^3 \\ +T\left[2J_1R\left(\frac{\ddot{\vartheta}_l T_2}{\eta}\right)_{mean} + (2Rk_v + k_bk_t)\left(\frac{\dot{\vartheta}_l T_2}{\eta}\right)_{mean}\right]\tau^2 \\ +hT_f\left(2Rk_v + k_bk_t\right)\tau + T\left[RJ_1^2\left(\ddot{\vartheta}_{l,RMS}\right)^2 + \left(Rk_v + k_bk_tk_v\right)\left(\dot{\vartheta}_{l,RMS}\right)^2\right] = 0 \end{aligned} \tag{24}$$

In practice, such a formula cannot be adopted since it requires the knowledge of many parameters which, actually, depend on τ. Hence, the computation of the derivative $dE_{tot}/d\tau$ should consider the effect of τ on all the parameters. This problem could be tackled by iterating the design; however, iterative or combinatorial approaches have very small chances of meeting the optimal design due to the problem complexity.

Usually the gearbox size is chosen first, and then the choice of the motor is performed together with the transmission ratio. The resulting design is checked for feasibility and, when needed, the design procedure is iterated to search for a better option [27]. This commonly performed procedure has some limitations: first of all, a sequential choice of the gearbox and of the motor is not always the best option, since the motor characteristics are unknown when choosing the reduction gear ratio. Another limitation is that this design procedure is not explicitly tailored for energy minimization, as the common design objective is the minimization of the motor size (and cost).

To find a feasible and optimal design in a clear, quick and efficient manner, the number of variables that appear in equations (13,21,23) must be reduced. The next section will highlight how scaling rules can be defined to model each component of the system and then how they can be used to express the overall

This is a pre-print of the article: P. Boscariol, D. Richiedei
Energy optimal design of servo-actuated systems: a concurrent approach based on scaling rules
Renewable and Sustainable Energy Reviews, Volume 156, March 2022, 111923
https://doi.org/10.1016/j.rser.2021.111923

energy consumption according to just two 'governing parameters': the motor continuous torque at stall, T_{CS}, and to the transmission ratio τ.

4 Use of scaling rules

4.1 Introduction to scaling rules

The aim of this section is to provide a basic introduction to the use of scaling rules for the design of a servo-actuated system, and to show the development of the scaling rules for all the elements involved in the design of the system under investigation.

Scaling rules (or scaling laws, equivalently) are metamodels representing the functional relationship that occurs between two physical quantities that scale over each other. Scaling rules allow simplifying the task of finding the relationship between some physical parameters of a given object, that can be very useful when physics-based models are of impractical use for their complexity or they are unavailable [21].

The use of scaling rules in a design problem can be very advantageous since it allows reducing the number of design parameters needed to capture the phenomena under investigation. The method of scaling rules is rooted into Buckingham's theorem [28, 29], which states that a physical equation involving n parameters and k physical dimensions can be rewritten in terms of $p = n - k$ parameters, usually indicated as $\pi_1, \pi_2, \ldots, \pi_p$. The usefulness of Buckingham's theorem lies not only on the reduction of the number of parameters involved in the description of some physical quantity, but also in the capability of computing such set of parameters even if the underlying physical model is unknown. It should be pointed out also that, in general, the choice of the set of parameters is not unique, so the user can sometimes choose one set of parameters over another just for convenience. Therefore, one quantity can often be expressed by more than one scaling rule without any loss in accuracy.

The use of scaling rules as a powerful tool for the analysis, the design and the optimization of electromechanical devices follows a well-established tradition, as several examples can be found in literature, with applications to robotic systems [30, 31], motors [32, 33], reduction gears [32, 34] and other devices, such as drones [35] or gas turbines [36], just to cite few examples.

As far as the development of scaling rules is concerned, they can be inferred from analytic relations as well as from experimental data: in this work the two methods are, when possible, combined. In the absence of a tractable analytic model, the primary source of evaluation (and validation) of the scaling rules is the experimental data contained in manufacturer's catalogs, which represent an invaluable sources of data for the designers. The analysis proposed in the following will involve the four main components of a servo-motor unit, i.e. the motor, the gearbox, the coupling and the motor drive.

This is a pre-print of the article: P. Boscariol, D. Richiedei
Energy optimal design of servo-actuated systems: a concurrent approach based on scaling rules
Renewable and Sustainable Energy Reviews, Volume 156, March 2022, 111923
https://doi.org/10.1016/j.rser.2021.111923

4.2 Motor scaling rules

4.2.1 Motor moment of inertia

The scaling of the motor moment of inertia can be performed, as suggested by Budinger et. al. in [37], using the nominal motor torque as the reference parameter, so that $J_m \propto T_m^{5/3}$. Nominal motor torque is, again as suggested in [21], proportional to the mass, which, in turn is proportional to the third power of the colorredadimensional ratio l^* (defined as the ratio between the actual motor length and a reference motor length), and inertia is proportional to ${l^*}^5$, if rotor radius and lengths have the same scaling. Therefore, $J_m \propto T_m^{5/3}$. Actually, the value assumed by the nominal motor torque depends on the choice of the rated speed that can be different for motors with the same size (and hence equal J_m); therefore, the relation should be corrected to account for such a speed. A more effective representation, that does not depend neither the choice of the rated speed, nor on other speed constraints, is provided if the governing parameter is the motor continuous torque T_{CS} [20] at stall (i.e. at zero speed):

$$J_m = a_m T_{CS}^{5/3} \tag{25}$$

The parameter T_{CS} is available in every manufacturer's catalog, and can be used to rank the size of the motor. This scaling rule, as well as the other ones that will be presented in Section 4.2, are tested against the experimental data provided by the manufacturer Kollmorgen, referring the brushless motors belonging to the 'AKM' family (having 400 V excitation), which are available through the manufacturer's webpage `www.kollmorgen.com`. The set of motors taken into consideration includes include 59 motors with nominal sizes ranging from 0.84 Nm to 25.03 Nm. Other groups of motors and other manufacturers can be chosen as well without altering the notation, as the data representation in catalogs is quite consistent among different manufacturers.

The value of the proportionality constant a_m in eq. (25) is found by interpolation of such data, using a least square routine. The value $a_m = 1.9657 \cdot 10^{-5} \ \frac{kg\, m^{1/3}}{N}$ provides a very good fit, as the correlation coefficient is found to be $R = 0.9858$. A direct comparison between the theoretical fit and the actual data is shown in Figure 2: the red line is the value of the fitting function according to eq (25), the black circles are the data extracted from the catalog.

4.2.2 Motor constant

Rather than developing a separate scaling rule for the equivalent armature resistance, R, and for the torque constant k_t, a simpler and more precise scaling rule can be developed for the ratio R/k_t^2, which appears in eq. (13). The inverse of this ratio, k_t^2/R, is often referred to as the square value of the 'motor constant' k_M. In [38], it is shown that the motor constant can be parametrized by the gap radius, i.e. the radial measure of the air gap between rotor and stator. In particular, the ratio k_t^2/R is proportional to r_{gap}^3. On the other hand, always according to the same source, the motor inertia is proportional to the third

This is a pre-print of the article: P. Boscariol, D. Richiedei
Energy optimal design of servo-actuated systems: a concurrent approach based on scaling rules
Renewable and Sustainable Energy Reviews, Volume 156, March 2022, 111923
https://doi.org/10.1016/j.rser.2021.111923

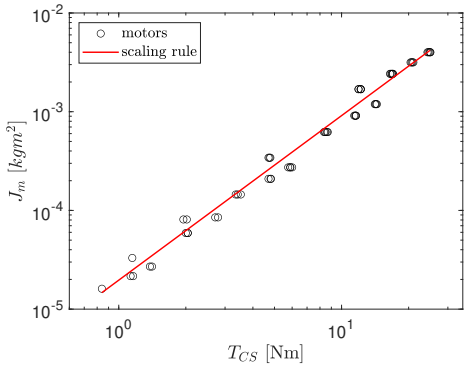

Figure 2: Motor inertia: scaling rule vs. actual data

power of r_{gap}: $J_m \propto r_{gap}^3$. Hence, R/k_t^2 can be parametrized using the same 'five-third' proportionality to T_{CS} already highlighted for the motor inertia in eq.(25):

$$\frac{R}{k_t^2} = \frac{a_{Rkt}}{T_{CS}^{5/3}}$$

where a_{Rkt} is the proportionality constant. The application of the proposed scaling rule to the catalog data leads to the almost unitary correlation coefficient $R = 0.9999$ obtained by setting $a_{Rkt} = 36.1225\ \frac{\Omega A^2}{Nm^{1/3}}$, hence proving the accuracy of this scaling rule. The fitting is shown in figure 3.

The fact that as T_{CS} increases, the ratio R/k_t^2 decreases with the same trend of the increase of J_m, has a relevant impact on the motor energy consumption. Motors with high T_{CS} must provide more torque to compensate for their higher inertia, but the effect of such high torques on the energy consumption is counterbalanced by a smaller armature resistance and a smaller ratio R/k_t^2.

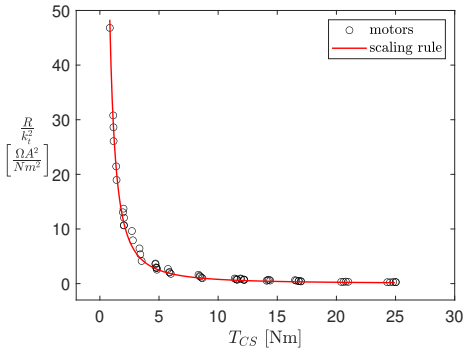

Figure 3: Ratio R/k_t^2: scaling rule vs. actual data

A second ratio is to be evaluated: the value of the ratio between the back-

This is a pre-print of the article: P. Boscariol, D. Richiedei
Energy optimal design of servo-actuated systems: a concurrent approach based on scaling rules
Renewable and Sustainable Energy Reviews, Volume 156, March 2022, 111923
https://doi.org/10.1016/j.rser.2021.111923

emf constant and the torque constant, k_b/k_t, that is required to compute the mechanical energy loss according to eq.(21). Such a ratio depends on the motor type and on its excitation, and it is independent from the motor size. Hence, no specific scaling rules are needed here.

4.2.3 Motor friction

The power dissipation in a brushless motor due to friction takes place mostly in the ball bearing used to counteract the forces acting on the motor shaft. Another source of mechanical dissipation is due to windage losses, which are caused by the friction between the rotor and the surrounding air. The modeling of such a loss is rather complex, since it involves the determination of the correct Reynold number according to the air flow conditions as well as other parameters whose estimation is not possible without a detailed model of the motor under consideration [39]. Given that the rotor surface in a brushless motor is quite smooth and has a cylindrical shape, such windage losses can be estimated to be rather small.

There is a general consensus on modeling friction torque in roller bearings as a speed-dependent phenomenon, as testified in several works such as [40, 41]. Such speed-dependence is usually described through a static friction torque and a constant viscous friction coefficient. More complex models can be used [42], but given the difficulty of providing a truly accurate description of friction under wildly varying conditions, the two terms model friction seems accurate enough. Moreover, the manufacturer's datasheets that are used as a reference in this work provide, at most, friction data as a Coulomb torque, T_f, and a viscous friction coefficient k_v.

Friction losses in ball bearings are directly proportional to the load acting on them [43]: in a well-designed application the motor bearing should counteract the weight of the rotor and the inertial forces due to the rotor unbalance, which can be traced back to the rotor moment of inertia. Since the latter is, as shown in eq.(25), proportional to $T_{CS}^{5/3}$, static friction is reasonably obeying to the same scaling law. The following scaling law is therefore proposed for the static friction torque:

$$T_f = a_t T_{CS}^{5/3} + b_t \tag{26}$$

The constant term b_t is added to provide a better fit for smaller size motors. Fitting the available data with the law in eq.(26) provides a correlation coefficient $R = 0.9847$ for $a_t = 8.4951 \cdot 10^{-4}\ Nm^{-2/3}$ and for $b_t = 0.0130\ Nm$, and the comparison between the actual and the fitted data is shown in figure 4.

Viscous friction in ball bearings is only slightly influences by the load [41], being mostly affected by the viscosity of the lubricant medium. Nonetheless, the data available in the manufacturer's datasheet show a direct proportionality between the viscous friction coefficient k_v and the motor size, that is well fitted by the linear scaling law:

$$k_v = a_v T_{CS} \tag{27}$$

This is a pre-print of the article: P. Boscariol, D. Richiedei
Energy optimal design of servo-actuated systems: a concurrent approach based on scaling rules
Renewable and Sustainable Energy Reviews, Volume 156, March 2022, 111923
https://doi.org/10.1016/j.rser.2021.111923

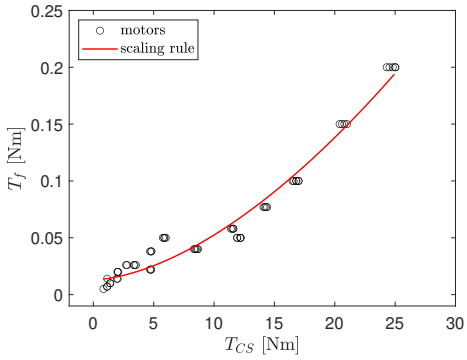

Figure 4: Motor static friction torque T_f: scaling rule vs. actual data

The fitting of the scaling rule to the manufacturer's data is shown graphically in fig. 5: the correlation coefficient is $R = 0.9792$ for $a_v = 3.815 \cdot 10^{-5}\ s/rad$.

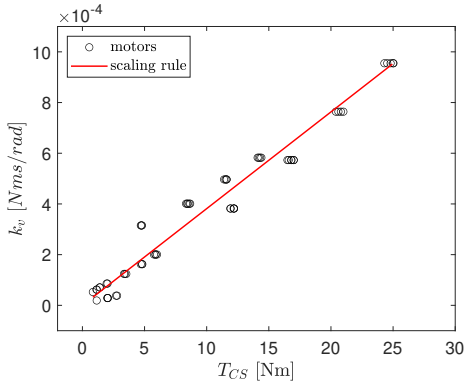

Figure 5: Motor viscous friction constant: scaling rule vs. actual data

4.2.4 Continuous torque limit

The characteristic curve of a brushless motor is usually represented as shown in fig. 6. The diagram in fig. 6 highlights two main areas: the intermittent zone and the continuous zone. The first one is upper bounded by the peak stall torque T_{PS} up to the knee speed ω_k, and then by the tension limit up to $\omega_{m,max}$, which is the absolute maximum speed of rotation of the motor shaft. The intermittent zone is then lower bounded by a speed-dependent continuous torque limit that is equal to T_{CS} at stall, and decreases with speed. This torque limit is usually approximated as a straight line with a negative slope. The intermittent zone represents the working conditions that the motor can withstand for short time intervals. As for the continuous zone, shown in gray color in fig. 6, the motor can operate within such an area for infinite time without exceeding the limit

This is a pre-print of the article: P. Boscariol, D. Richiedei
Energy optimal design of servo-actuated systems: a concurrent approach based on scaling rules
Renewable and Sustainable Energy Reviews, Volume 156, March 2022, 111923
https://doi.org/10.1016/j.rser.2021.111923

temperature.

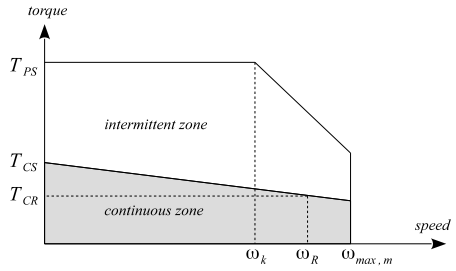

Figure 6: Brushless motor characteristic curve

The negative slope of the T_{CS} limit as a function of the motor speed is here denoted by the symbol δ and inferred from the motor characteristic curve as:

$$\delta = \frac{T_{CS} - T_{CR}}{\omega_R} \tag{28}$$

Hence, the speed-dependent continuous torque limit can be expressed as:

$$T_C(\dot{\vartheta}_{m,RMS}) = T_{CS} - \delta\dot{\vartheta}_{m,RMS} \tag{29}$$

Since the values of T_{CS} and T_{CR} are available in all motor datasheets, δ can be easily estimated from manufacturer's data.

The parameter δ can be also represented through a scaling rule as a function of the main motor sizing parameter, T_{CS}. Observing the data taken from the manufacturer's catalogs, δ appears to be directly proportional to the motor size, since the losses in the motor and the viscous friction coefficient increase almost linearly with the magnetic induction [44, 20]. As such, the following scaling rule is proposed:

$$\delta = a_\delta T_{CS} \tag{30}$$

This scaling rule provides a good fit with the experimental data supplied in the catalogue adopted in this work as shown in figure 7. The optimal fitting is found for $a_\delta = 7.8268 \cdot 10^{-4}\ s/rad$, with a correlation coefficient $R = 0.9690$.

4.2.5 Motor minimum size

The minimum sizing of the motor is defined by taking into account the characteristic curve of the motor, which is usually shaped as in fig. 6 for brushless motors and DC motors.

Motor sizing for non-intermittent operation is based on the just discussed continuous torque limit $T_C(\dot{\vartheta}_m)$, and the following inequality must hold [20]:

$$T_C(\dot{\vartheta}_{m,RMS}) \geq \alpha_s T_{m,RMS} \tag{31}$$

This is a pre-print of the article: P. Boscariol, D. Richiedei
Energy optimal design of servo-actuated systems: a concurrent approach based on scaling rules
Renewable and Sustainable Energy Reviews, Volume 156, March 2022, 111923
https://doi.org/10.1016/j.rser.2021.111923

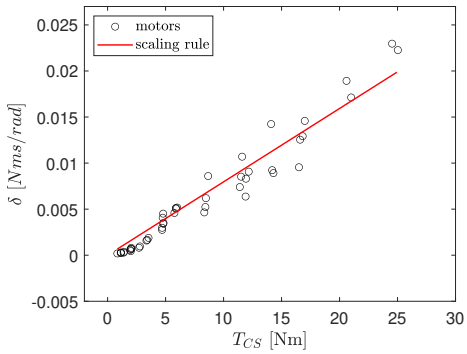

Figure 7: δ: scaling rule vs. actual data

where α_s is safety factor (greater than 1 and usually no smaller than 1.2 [20]), $T_{m,RMS}$ and $\dot{\vartheta}_{m,RMS}$ are the RMS value of the motor torque and speed respectively, to be computed as follows:

$$T_{m,RMS} = \sqrt{\frac{\int_0^T T_m^2(t)dt}{T}} \tag{32}$$

$$\dot{\vartheta}_{m,RMS} = \sqrt{\frac{\int_0^T \dot{\vartheta}_m^2(t)dt}{T}} \tag{33}$$

Using equations (29,30) in eq.(31) returns the minimum sizing of the motor, according to the motor RMS speed and torque as:

$$T_{CS,min} = \frac{1}{\alpha_s} \frac{T_{m,RMS}}{1 - \alpha_\delta \dot{\vartheta}_{m,RMS}} \tag{34}$$

4.3 Gearbox scaling rules

The relevant parameters of the gearbox are the transmission ratio τ, the gearbox moment of inertia J_r, and its efficiency, η.

4.3.1 Gearbox moment of inertia

In [21, 37] it is suggested that the moment inertia of a planetary gearbox can be represented by relating it to the nominal torque that the gearbox can withstand. This is assumed according to the principle that a gearbox is designed by focusing on mechanical stress, which must be kept below elastic or fatigue limits [45]. Hence, the gearbox inertia can be related to the five-third power of its nominal torque. In [20], and further corroborated in this work, it is shown that the gearbox inertia should be related to the reduction ratio τ too, since the desired gear ratio is set by setting the proper number of teeth for each element of the transmission. Again, the number of stages should be accounted for as well.

This is a pre-print of the article: P. Boscariol, D. Richiedei
Energy optimal design of servo-actuated systems: a concurrent approach based on scaling rules
Renewable and Sustainable Energy Reviews, Volume 156, March 2022, 111923
https://doi.org/10.1016/j.rser.2021.111923

The relation between J_r and τ is the most important to be accounted for, given the goal of this work. Indeed, the required rated torque of the gearbox is computed at the early stages of the design, regardless of the selection of τ and of the motor, on the basis of the desired motion of the load and the estimated load-side external forces [20]. Additionally, manufacturers usually supply gearboxes with similar values of the rated torque, with different gear ratio. Hence, when τ and the motor are to be chosen, the size (i.e. the rated torque) of the gearbox has been already identified. If gearboxes with the same size (i.e. with almost identical rated torque) are considered, the gearbox moment of inertia can be related to τ by the following scaling rule:

$$J_r = a_r + b_r \tau^{c_r} \tag{35}$$

in which the coefficients a_r, b_r and c_r are coefficients to be obtained through a proper fitting of the experimental data provided by manufacturers. If gearboxes with different number of stages are considered, the scaling rule is a discontinuous function of τ and Eq.(35) is locally defined for a specified number of stages.

Looking at the technical data from the gearbox manufacturer's catalogue [11] assumed as the test case, it can be noticed the that within the same size, among all 7 sizes available, all the single stage reducers have the same mass, but they vary in moment of inertia as τ changes; the same applies to double-stage reducers. This scaling rule has been tested for several gearbox sizes: the results for the SP100+ MF and for the SP140+ MF sizes is shown in figure 8. The scaling parameters must be defined by distinct values for each size and for each configuration, i.e. for single and for dual stage gearboxes. The fitting for SP100+ MF gearboxes provides the following values:

$$a_{r1} = 8.1339 \cdot 10^{-4}\ Nm; \qquad b_{r1} = 8.4378 \cdot 10^{-4}\ Nm;$$

for single stage gearboxes, and the following ones for two-stage reducers:

$$a_{r2} = 1.6720 \cdot 10^{-4}\ Nm; \qquad b_{r2} = 4.6258 \cdot 10^{-4}\ Nm;$$

all being evaluated by setting $c_r = 1$. In the first case the correlation coefficient is $R = 0.9790$, in the second case a similar correlation coefficient is found: $R = 0.9667$. Focusing on the bigger size, i.e. on SP140+ MF, the scaling parameters for single and dual stages configurations are:

$$a_{r1} = 2.1491 \cdot 10^{-3}\ Nm; \qquad b_{r1} = 2.2547 \cdot 10^{-3}\ Nm;$$

$$a_{r2} = 8.7681 \cdot 10^{-4}\ Nm; \qquad b_{r2} = 2.1929 \cdot 10^{-3}\ Nm;$$

Again, such coefficients have been evaluated for $c_r = 1$, and the respective correlation coefficients are $R = 0.9805$ and $R = 0.9550$. The good accuracy of the scaling rule is shown graphically in figure 8 for all four groups under consideration.

This is a pre-print of the article: P. Boscariol, D. Richiedei
Energy optimal design of servo-actuated systems: a concurrent approach based on scaling rules
Renewable and Sustainable Energy Reviews, Volume 156, March 2022, 111923
https://doi.org/10.1016/j.rser.2021.111923

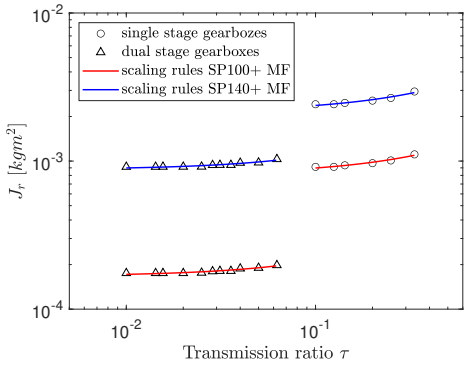

Figure 8: Gearbox inertia: scaling rule vs transmission ratio τ

4.3.2 Gearbox efficiency

As far as the gearbox efficiency is concerned, the datasheet provide just two values of estimated direct efficiency that apply to either single or dual stage ones. This data suggest that the efficiency is not affected by the transmission ratio, or at most the data used to compute η shows a minor dependence on τ. Therefore the efficiency must be modeled solely focusing on the number of stages.

The gearbox catalogs do not provide any information on reverse power flow efficiency, therefore the following commonly used formula [46, 20] is a adopted to estimate reverse power flow efficiency from the direct one:

$$\eta_r = 2 - \frac{1}{\eta_d} \tag{36}$$

The following typical efficiency values are provided in the catalogue under consideration:

$$\eta_d = 0.97 \quad \text{for single-stage reducers} \tag{37}$$

$$\eta_d = 0.94 \quad \text{for dual-stage reducers} \tag{38}$$

4.4 Scaling rule of the coupling

The sizing of the coupling that connects the motor and the gearbox input shaft should be performed to ensure that the coupling can withstand the peak torque to be transmitted. The peak torque acting on the coupling can be estimated as the maximum value of the torque acting the high-speed shaft, T_1. Therefore the sizing rule for the choice of the coupling can be written as:

$$T_{kn} \geq max|T_1|f_{ks} \tag{39}$$

where f_{ks} is the so-called shock factor, a safety coefficient that accounts for the shocking or impulsive characteristic of the load, and T_{kn} is the coupling

This is a pre-print of the article: P. Boscariol, D. Richiedei
Energy optimal design of servo-actuated systems: a concurrent approach based on scaling rules
Renewable and Sustainable Energy Reviews, Volume 156, March 2022, 111923
https://doi.org/10.1016/j.rser.2021.111923

rated torque, which is found on manufacturer's catalogs. The maximum value of T_1 can be estimated as the peak value of the load torque plus the maximum value of the inertial load, as in the formula:

$$max|T_1| \approx \frac{T_2^{max}}{\eta}\tau + \frac{J_r \ddot{\vartheta}_l^{max}}{\tau} \tag{40}$$

Since larger couplings are needed to withstand larger torques, the moment of inertia of the coupling J_c increases with the peak torque T_{kn} with the following scaling rule:

$$J_c = a_c T_{kn}^{b_c} \tag{41}$$

The theoretical value of b_c is equal to 5/3: indeed, the axial moment of inertia of a cylindrical element, as the coupling usually is, is proportional to the fifth power of its radius, while its resistance to torsional loads is proportional to the third power of its radius.

Combining equations (41) and (40) provides the scaling rule of the coupling moment of inertia as:

$$J_c = a_c f_{ks}^{5/3} \left(\frac{T_2^{max}}{\eta} + \frac{J_r \ddot{\vartheta}_l^{max}}{\tau} \right)^{5/3} \tag{42}$$

This scaling rule has been used to fit the data available from the datasheet of the BKL series coupling provided by the manufacturer $R+W$ America and available in [47], focusing on a wide range of sizes that spans rated torque values in the 2 to 500 Nm range. The fitting according to the 5/3 power of T_{kn}, as defined in eq.(39), provides a very good accuracy, as shown in figure 9 and as testified by the almost unitary correlation coefficient $R = 0.9983$ obtained by setting $a_c = 4.2707 \cdot 10^{-7}\ \frac{kg\,m^2}{Nm^{5/3}}$.

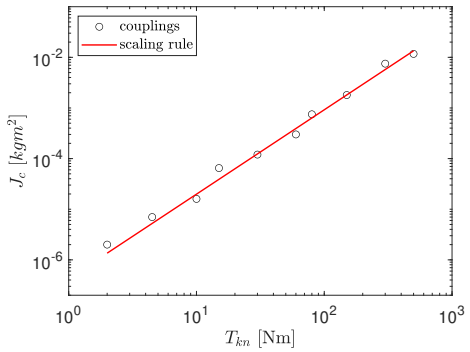

Figure 9: Coupling inertia: scaling rule vs maximum torque load T_{kn}

This is a pre-print of the article: P. Boscariol, D. Richiedei
Energy optimal design of servo-actuated systems: a concurrent approach based on scaling rules
Renewable and Sustainable Energy Reviews, Volume 156, March 2022, 111923
https://doi.org/10.1016/j.rser.2021.111923

4.5 Scaling of the motor driver efficiency

The overall energy consumption of the system is affected also by the dissipation in the motor drive circuit. The motor drive circuit is composed by two main elements: a three-phase rectifier and a three-legged half-bridge inverter. Modeling their efficiency is a complex task, which is in this case exacerbated by the lack of specific technical data from the manufacturer's datasheet. A simple, but still effective model is therefore needed. A basic solution is to take into account a constant efficiency η_{driver}, as commonly done when specific data are unavailable [8]. A more detailed model can be inferred by taking into account the dependency of η_{driver} on the load and by accounting for both rectifier losses and inverter losses. As shown experimentally in [48], the efficiency of the rectifier is strongly affected by the load, according to a law that can be approximated by an exponential, which can be used to represent the wide variation from the very low efficiency at light loads to the almost unitary efficiency at full load.

Inverter losses are more mildly affected by the load, but they follow a similar trend [49]. Accordingly, the efficiency of the load can be be parametrized by the drive load rate λ_{dr}, defined as the ratio between its actual current output and its maximum current output rating:

$$\eta_{driver} = \eta_{max} \left(1 - \exp(\sigma_{dr} \lambda_{dr})\right) \tag{43}$$

This model can be easily used to fit any typical driver efficiency curve: by choosing $\eta_{max} = 0.95$ and $\sigma_{dr} = 10$, the resulting load-dependent efficiency is shown in figure 10. The driver efficiency is very poor for light loads, but as soon as the load rate reaches 25%, η_{driver} is larger than 85% and at maximum load it is equal to the reasonable figure of 95%.

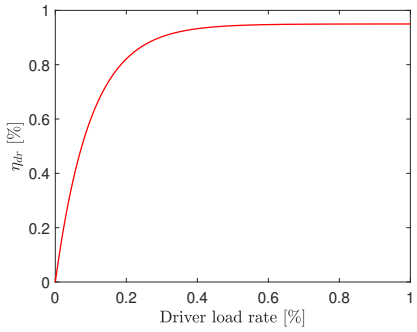

Figure 10: Estimated driver efficiency

The efficiency of drives is generally maximum when the current provided to the motor is close to their nominal current rating. Taking into account this efficiency model over a simpler constant efficiency has the advantage of discouraging the choice of oversized motors and drivers, which would operate at light loads and therefore far from their energy-wise optimal rating. An oversized

This is a pre-print of the article: P. Boscariol, D. Richiedei
Energy optimal design of servo-actuated systems: a concurrent approach based on scaling rules
Renewable and Sustainable Energy Reviews, Volume 156, March 2022, 111923
https://doi.org/10.1016/j.rser.2021.111923

motor is one for which its size is larger than the one required by the application. Since motor size is primarily dictated by the continuous service torque T_{CS}, and assuming that the motor driver is properly sized for the motor which he drives, the duty cycle of the driver can be represented by the $T_{CS,min}/T_{CS}$ ratio, being $T_{CS,min}$ the minimum allowed motor size for the application. Equation (34) can therefore be used to estimate the load rate of the motor driver, λ_{dr}, as:

$$\lambda_{dr} = \frac{T_{CS,min}}{T_{CS}} = \frac{\alpha_s T_{m,RMS}}{T_{CS}\left(1 - \alpha_\delta \dot{\theta}_{l,RMS}/\tau\right)} \tag{44}$$

This equation completes the definition of the scaling rules of all the relevant components of a servo-actuated system: all the scaling rules refer either to the motor continuous torque T_{CS} or to the gear ratio τ. Therefore, a complete parametrization of the design by just two values has been developed.

5 Energy-optimal design procedure

5.1 Formulation of the energy consumption

The reduction of design parameters to just T_{CS} and τ can now be exploited to express the overall energy consumption, as captured by equations (19-22-23), in term of them. Using the several scaling rules provided in Section 4 into eq.(23) leads to the following expression of the motor electric consumption:

$$\begin{aligned} E_m(T_{CS},\tau) = \Bigg[& \left(\frac{T_2\ddot{\vartheta}_l}{\eta}\right)_{mean} + 2J_1 + \tau^2 \left(\frac{T_2}{\eta}\right)^2_{RMS} + \left(a_t T_{CS}^{bc} + b_t\right)^2 \\ & + \frac{J_1}{\tau^2}\ddot{\vartheta}^2_{l,RMS} + 2a_v T_{CS}\left(\frac{T_2\dot{\vartheta}_l}{\eta}\right)_{mean} + 2\tau\left(a_t T_{CS}^{bc} + b_t\right)\left(\frac{T_2}{\eta}\right)_{mean} \\ & + \frac{a_v^2 T_{CS}^2 + \dot{\vartheta}^2_{l,RMS}}{\tau^2} + \frac{2a_v\, T_{CS}\, \left(a_t T_{CS}^{bc} + b_t\right)}{\tau\, T}\Bigg] \frac{T\, a_{kt}}{T_{CS}^{bc}} \\ & + \left[h\,\tau\left(a_t\, T_{CS}^{bc} + b_t\right) + T\left(\frac{T_2\dot{\vartheta}_l}{\eta}\right)_{mean} + a_v\, T\, \dot{\vartheta}^2_{l,RMS} T_{CS}\right] \frac{k_b}{k_t}\frac{1}{\tau^2} \end{aligned} \tag{45}$$

with:

$$J_1(\tau) = a_r + b_r\tau + T_{CS}^{bc} a_m + a_k\left(\left(\frac{T_2}{\eta}\right)\tau + \frac{\ddot{\vartheta}_{l,max}}{\tau}\left(a_r + b_r\tau\right)\right)^{bc} \tag{46}$$

To include the effect of the load-dependent driver efficiency too, eq.(44) should be used in eq.(23), leading to the following expression of the overall energy consumption:

This is a pre-print of the article: P. Boscariol, D. Richiedei
Energy optimal design of servo-actuated systems: a concurrent approach based on scaling rules
Renewable and Sustainable Energy Reviews, Volume 156, March 2022, 111923
https://doi.org/10.1016/j.rser.2021.111923

$$E_{tot}(T_{CS},\tau) = \eta_{max}\left(1 - \exp\frac{\sigma_{dr}\alpha_s T_{m,RMS}}{T_{CS}\left(1-\alpha_\delta \dot{\theta}_{l,RMS}/\tau\right)}\right) E_m\left(T_{CS},\tau\right) \quad (47)$$

The overall energy consumption is, again, a function of the two sizing parameters T_{CS} and τ, and of several size-independent scaling factors and constants taken from the catalogues. Hence, $E_{tot} = E_{tot}(T_{CS},\tau)$ can be evaluated, plotted and optimized within a complete sizing procedure, as shown in detail in the next section.

5.2 System sizing procedure

The energy-optimal, concurrent choice of motor, coupling and gearbox according to the method proposed in this paper, requires, first of all, the analysis of the component catalogues to define the scaling rule constants. This analysis can be performed according to the models presented in section 4 and through standard least-square data fitting routines. Then the steps to be followed to produce an energy-optimal design are listed in the following points.

1. Evaluation of the load-side conditions to estimate $T_2(t)$, on the basis of the chosen load-side motion profile as $\dot{\vartheta}_l(t)$, $\ddot{\vartheta}_l(t)$. These profiles are then used to evaluate their mean, RMS and peak values.

2. Selection of the gearbox size according to the peak output torque and the rated torque [27]. As for the peak torque, the following constraint should be considered:
$$T_{2B} > T_2^{max} f_s \quad (48)$$
meaning that the peak torque rating of the gearbox, T_{2B}, must be larger than the maximum value of the load-side torque T_2^{max}, including the service factor f_s to account for the specific field of application and for the number of working cycles per hour, according to the specific gearbox manufacturer's suggestions. This limit is independent of τ and of the motor size, and therefore it can be enforced at this early stage without the need of any iteration. As for the gearbox rated torque T_{2R}, the following constraint should be considered as well to chose the correct gearbox size, after computing the root mean cubic value of T_2 as $T_{2,RMC}$:
$$T_{2R} > T_{2,RMC} = \sqrt[3]{\frac{\int_0^T |T_2^3(t)\dot{\vartheta}_l(t)|dt}{\int_0^T |\dot{\vartheta}_l(t)|dt}} \quad (49)$$
As the previous one, this constraint is independent of τ and of the motor choice.

This is a pre-print of the article: P. Boscariol, D. Richiedei
Energy optimal design of servo-actuated systems: a concurrent approach based on scaling rules
Renewable and Sustainable Energy Reviews, Volume 156, March 2022, 111923
https://doi.org/10.1016/j.rser.2021.111923

3. Synthesis of the scaling rules for the gearbox within the selected size, for the coupling, for the motor and for the drive.

4. Minimization of the energy consumption, by defining the optimal choices of T_{CS} and τ as those minimizing the cost function of eq.(47). The minimization problem can be stated as:

$$\min_{[T_{CS},\tau]} \quad E_{tot}(T_{CS},\tau) \tag{50}$$

$$\text{subject to:} \quad \tau > \max\left\{\frac{|\dot{\vartheta}_l|_{max}}{\omega_{1B}}, \frac{\int_0^T |\dot{\vartheta}_l(t)|dt}{\omega_{1,r}\,T}, \frac{|\dot{\vartheta}_l|_{max}}{\omega_{m,max}}\right\} \tag{51}$$

$$\text{subject to:} \quad T_{CS} > \frac{1}{\alpha_s}\frac{T_{m,RMS}}{1-\alpha_\delta \dot{\vartheta}_{m,RMS}} \tag{52}$$

The constraint in eq.(51) is introduced to account for the speed limitations of the gearbox, to comply with its absolute maximum speed ω_{1B} and for its rated speed, $\omega_{1,r}$, both referred to the input shaft, and to account for the motor maximum speed $\omega_{m,max}$. These constraints are to be enforced at this stage of the design procedure, as they have an obvious dependency on τ. The constraint in eq.(52) that represents the minimum motor size has already been discussed in section 4.5. Other constraints can be set as well, such as constraints on the inertia ratio.

5. Selection of the gearbox, among the selected size of the adopted catalogue, by identifying a close match to the optimal gear ratio

6. Selection of the motor from the adopted catalogue, by identifying a close match to the optimal motor sizing T_{CS} and a reasonable value of maximum speed, when more than one option is available.

7. Verification of the designed system with the actual data provided by manufacturers.

6 Application example I: integrated design of a constant inertia system

In this first example the proposed method for the energy-optimal design is applied to a constant inertia system, with the aim of providing a description of the just outlined step-by-step procedure in the clearest possible manner. The choice of the components is limited to the data-sheets used for the definition of the scaling rules constants, although the method can be applied with reference to other databases of components as well.

In this first test case, the load is made by a constant inertia load, $J_L = 2$ kgm^2, plus a constant resistant torque $T_e = 4$ Nm and a friction torque with viscous constant $k_f = 2 \times 10^{-2}$ $Nm\,s/rad$. The sample motion assumed for the load consists of a rotation h equal to 10 revolutions, which takes place over a

This is a pre-print of the article: P. Boscariol, D. Richiedei
Energy optimal design of servo-actuated systems: a concurrent approach based on scaling rules
Renewable and Sustainable Energy Reviews, Volume 156, March 2022, 111923
https://doi.org/10.1016/j.rser.2021.111923

motion time equal to 5 s, followed by a pause lasting 2 s. The motion profile is a trapezoidal speed one, with acceleration and deceleration times equal to 1/10 of the motion time. These data completely specify the load-side conditions in terms of load side torque, $T_2(t)$ and $\dot{\vartheta}_l$. Both are represented by the graphs in fig. 11.

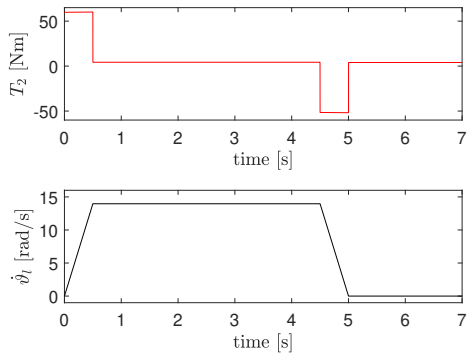

Figure 11: Test case I: load-side torque $T_2(t)$ and speed $\dot{\vartheta}_l(t)$ profiles

On the basis of the computed load-side torque and speed, a set of suitable gearboxes can be defined, according to the system sizing procedure presented in section 5. According the manufacturer's recommendation [11] a unitary safety factor f_s is used to evaluate the minimum admissible value of T_{2B} (see eq.(48)) since the number of cycles per hour is less than 1000: the minimum value of T_{2R} is then equal to 60.1 Nm. As far as rated output torque is concerned (eq.(49)), the minimum value is $T_{2R} = 27.1$ Nm. Hence, the single-stage and dual-stage gearboxes belonging to the SP+ 100 MF family are well suited for the application. The reducers belonging to the subsequent SP+ 140 MF size, as well as to the larger sizes, are oversized for the application and hence they are excluded from the design procedure.

The combination of the 17 gearboxes belonging to the SP+ 100 MF family (with $i = 1/\tau$ ranging from 3 to 100) with the 45 motors taken into consideration from the datasheet [50] leads to as many as 765 possible design to be evaluated, if an enumerative approach would be used.

Solving the optimization problem of eq.(50), gives the following results: the minimum energy consumption is equal to 297.9 J, obtained for $i = 9.4$ and $T_{CS} = 8.9$ Nm. The optimization routine is of quick and straightforward implementation and solution, given that the optimization problem is convex. The dependency of the energy consumption on i and on T_{CS} is highlighted by figure 12, which clearly shows the convexity of the energy function (just the single-stage gearboxes are shown for clarity of representation). The optimal design is represented by the black circle.

The optimal values of T_{CS} and τ resulting from the optimization can now be used to browse the motor and the reducer datasheets: the SP100+ catalog includes a reducer with $i = 8$, so this can be chosen for the design. As far as the

This is a pre-print of the article: P. Boscariol, D. Richiedei
Energy optimal design of servo-actuated systems: a concurrent approach based on scaling rules
Renewable and Sustainable Energy Reviews, Volume 156, March 2022, 111923
https://doi.org/10.1016/j.rser.2021.111923

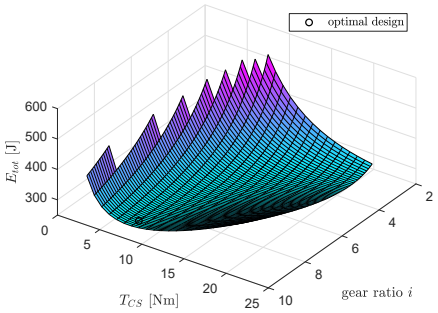

Figure 12: Energy consumption vs. reduction ratio i and motor size: model based on scaling rules

motor choice is concerned, the AKM52 motor class includes five motors with T_{CS} that ranges between 8.3 and 8.67 Nm, which are close to the predicted 'best' value of $T_{CS} = 8.9$ Nm. Any choice among the five candidate motors provides a similar overall energy consumption, so our choice is to pick the one whose maximum speed is close to the maximum speed required by the application, i.e. the AKM52E. Indeed, this choice leads to the feasible motor with the smallest power rating among the candidate motors. The resulting estimated energy consumption, computed using the actual parameters provided by the manufacturers in the datasheet, is equal to 303 J, which closely matches the prediction of the model based on scaling rules, thus further corroborating the correctness of the developed motors. The resulting inertia ratio, defined as the ratio of the reflected load inertia and the motor inertia, is equal to 50.1: such an high value might seem quite odd, but it complies with the experimental evidence of the motor manufacturer, described in the work [13] that refers to increasing the gear ratio as a mean to boost energy efficiency. The motor speed-torque pairs is shown in fig. 13(a) together with the motor characteristic curve and the RMS speed-torque pair, which is highlighted by the star-shaped marker.

Testing all the 270 possible design combinations using the actual catalog parameters, i.e. referring to the data shown in fig. 14 with reference to just single-stage gearboxes, highlights a slightly different energy-optimal design, found by using $i = 8$ and the motor AKM52L, which has a slightly larger T_{CS} (equal to 8.67 Nm) and higher speed capabilities than the previously chosen motor. The energy requirement for this design is equal to 299.4 J: the small improvement of energy efficiency from the previous design choice is however very limited (1.4%) and this design is, in practice, equivalent to the one found through the scaling rules. This corroborates that the proposed method is based on a reliable representation of the energy consumption that can replace the time-consuming and error-prone method of testing hundreds of design choice.

A further analysis of the energy-optimal design reveals that it leads to a sensibly larger motor than the smallest feasible one: the minimum size motor that complies with the limit of eq.(52) has a continuous stall torque $T_{CS} =$

This is a pre-print of the article: P. Boscariol, D. Richiedei
Energy optimal design of servo-actuated systems: a concurrent approach based on scaling rules
Renewable and Sustainable Energy Reviews, Volume 156, March 2022, 111923
https://doi.org/10.1016/j.rser.2021.111923

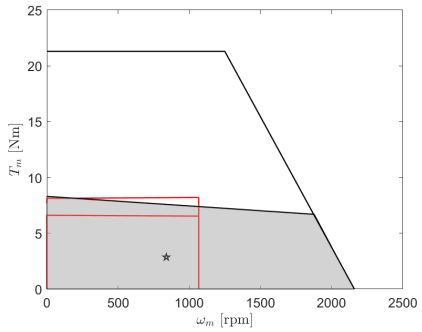

Figure 13: Characteristic curve and required speed-torque pairs for the motor AKM52E with $\tau = 1/8$. RMS operating point show by the black star

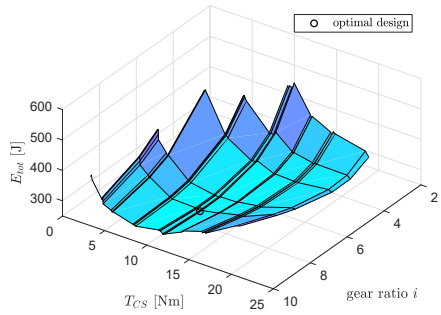

Figure 14: Energy consumption vs. reduction ratio i and motor size: model based on actual data

3.9 Nm which, coupled to a gearbox with $i = 8$, requires 384.4 J to execute one working cycle. This point is located on the bottom-left point of the surface shown in fig. 12. The closest (feasible) match to this motor size is the motor with $T_{CS} = 4.7\ Nm$ which requires as much as 398.2 J for each working cycle i.e. the increase of energy consumption is equal to +26.9%. Choosing the smallest size motor provides the cheapest purchase option of the motor, but is more expensive in the long run if the cost of the energy is taken into account as well. It is interesting noticing that the energy consumption provided by the minimum-torque design is higher, thus corroborating the effectiveness of the underlying idea of the proposed method. Generally speaking, a slight oversize of the motor together with the suitable gear ratio allows reducing the energy consumption despite the increase of the motor inertia. This is due to the beneficial effect of the motor-size increase on the reduction of the ratio R/k_t^2, that decreases with the same trend of the increase of J_m. Since R/k_t^2 affects the contributions on the energy absorbed by both the load side and the motor side, the overall energy is lowered despite the increase of J_m. On the other hand, excessive oversizing is

This is a pre-print of the article: P. Boscariol, D. Richiedei
Energy optimal design of servo-actuated systems: a concurrent approach based on scaling rules
Renewable and Sustainable Energy Reviews, Volume 156, March 2022, 111923
https://doi.org/10.1016/j.rser.2021.111923

prevented by the small efficiency of the drive when it works far from the rated current (see eq.(43,44)), and by the increase of the coupling moment of inertia as the motor-side torque increases (see eq.(42)).

7 Application example II: integrated design of a variable inertia system

The method outlined in this work, as already mentioned, can be applied to any load, including mechanical systems with variable inertia. One example is here provided by the slider-crank mechanism shown in fig. 15(a). The mechanism is modeled by taking into account the mass of the crank, of the slider and of the connecting rod, as well as the effects of gravity.

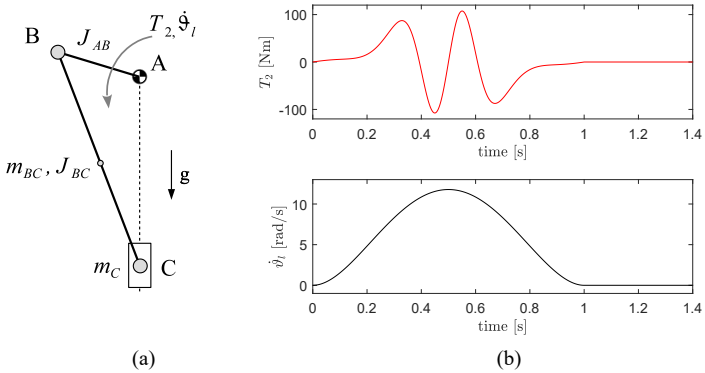

(a) (b)

Figure 15: Test case II - slider crank mechanism (a), load-side torque and speed profile (b)

The motion of the mechanism is represented by a fifth-degree profile of the crank angular position, which performs a full rotation in 1 s, followed by a 0.2 s rest phase. The resulting joint speed $\dot{\vartheta}_l(t)$ and torque acting on the gearbox shaft, $T_2(t)$, are shown in fig. 15(b).

The design of the energy-optimal actuation system for this system is, as in the previous test-case, first performed through the proposed method and then assessed through the evaluation of all the 354 possible design combinations. The gearbox sizing sets the requirements $T_{2B} > 136.3\ Nm$ and $T_{2R} > 69.8\ Nm$, leading to the choice of the class SP100+ of the adopted datasheet. Solving the constrained energy optimization problem results in an optimal design with $\tau_{opt} = 1/10$ and $T_{CS_{opt}} = 17.9\ Nm$, leading to the estimated energy consumption $E_{opt} = 27.3\ J$. Fig.16(a) shows the estimated energy as a function of τ and T_{CS} (two-stage reducers are neglected for a clearer representation) and the optimal design is highlighted by the black circle. The evaluation of the energy consumption of all the combinations of the single-stage reducers and all the

This is a pre-print of the article: P. Boscariol, D. Richiedei
Energy optimal design of servo-actuated systems: a concurrent approach based on scaling rules
Renewable and Sustainable Energy Reviews, Volume 156, March 2022, 111923
https://doi.org/10.1016/j.rser.2021.111923

motors is shown in fig.16(b): it is clear that fig.16(a) provides a very precise approximation of the actual absorbed energy.

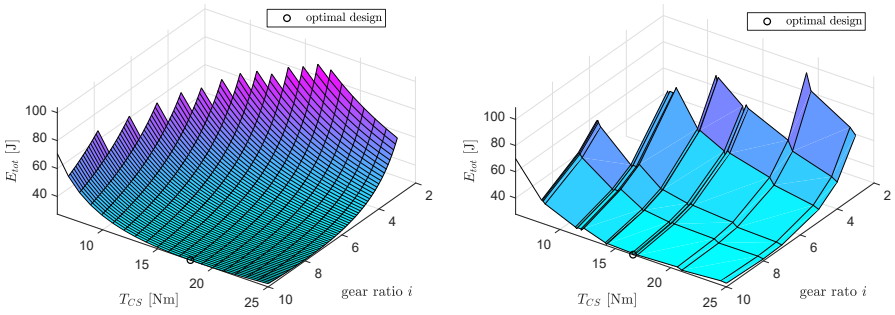

(a) Scaled data (b) Actual data

Figure 16: Test case II: sizing with single stages reducers

The AKM63 motor class, whose T_{CS} values range from 16.6 to 17 Nm, is the one that better fits the theoretical optimal design. Among the five motors in this class, the one with the smallest power rating is the AKM63G, whose T_{CS} is equal to 16.6 Nm and whose rated speed is equal to 1500 rpm, choosing this motor with a $10:1$ reducer results in an estimated energy consumption per cycle equal to 28.7 J, which is very close to the expected one. The characteristic curve of the AKM63G motor, the torque-speed pairs and the RMS operative point are shown in fig.17. As in the previous test-case, the motor is more than twice larger than the absolute minimum motor size design, which leads to the solution $\tau = 1/10$, $T_{CS} = 6\ Nm$.

Since the surface representing the energy vs. T_{CS} and τ in fig.16 is flat around the optimal value, a suboptimal (but still very good) design can be

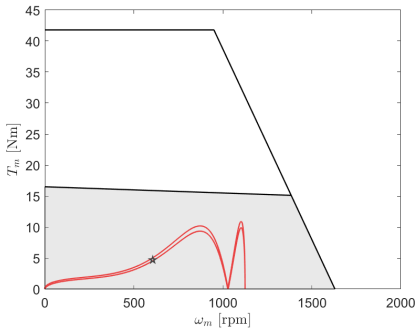

Figure 17: Test case II: torque-speed pairs for the AKM63G motor with $\tau = 1/10$

This is a pre-print of the article: P. Boscariol, D. Richiedei
Energy optimal design of servo-actuated systems: a concurrent approach based on scaling rules
Renewable and Sustainable Energy Reviews, Volume 156, March 2022, 111923
https://doi.org/10.1016/j.rser.2021.111923

obtained with a smaller motor, such as the AKM54G one, whose continous torque at stall is $T_{CS} = 14.3\ Nm$. The expected energy consumption, evaluated on the basis of the datasheet values, is slightly increased to 29.4 J i.e. by +2.4% in this case the lesser energy efficiency might be compensated by a cheaper initial cost.

8 Conclusions

This paper proposes an effective approach to the reduction of the energy consumption in servo-actuated mechanism by by means of the optimal selection of the motor and the gearbox. The problem has a relevant impact since these systems are widely adopted in modern industry, and designers usually just rely on off-the-shelf components using traditional sizing approaches that neglect the issue of energy consumption. The proposed method is based on the use of scaling rules, which condensate into simple relationships the properties of the relevant components of the system: the motor, the coupling and the planetary gearbox. Such metamodels can be easily obtained by the data provided in datasheets, thus making the proposed method simple to implement and appealing to the industry practitioner. In particular, the proposed scaling rules allow to refer all the relevant design data to just two governing parameters, i.e. the motor continuous torque at stall and the gear ratio. The core of the energy-optimal design is the analytic formulation of the overall energy consumption of the system which is performed by exploiting the scaling rules. As a result, the energy-optimal design can be set as a two-parameters constrained optimization problem.

The method is of general application, given that the design procedure is compliant with a generic load and the scaling rules can be fitted to any collection of manufacturers' data. The formulation of the scaling rules is here applied to planetary gearboxes, but analogous models can be developed for other devices as well.

The effectiveness and the accuracy of the design procedure is tested by applying it to two test-cases, showcasing the suitability to both constant and variable inertia loads. The results show that the approximation introduced by the use of scaling rules is rather minor, leading to a very precise estimation of the energy expenditure. Nonetheless, the proposed design method is simple and quickly leads to the optimal solution.

The two design examples included in this work show that the solution found by applying the proposed method is virtually identical to the optimal one in both cases, the latter being found by an exhaustive exploration of the design space, i.e. by testing, one by one, all the possible combinations of motors and reducers available in the catalogs. The results show some interesting features: first of all, a wise selection of the motor and of the transmission ratio allows for a relevant energy saving. Moreover, due to the relevant decrease of the motor winding resistance as the motor size increases, looking for the minimum-size motor is not always the best choice in term of energy consumption. The results also suggest that energy efficiency can be boosted by setting the inertia ratio

This is a pre-print of the article: P. Boscariol, D. Richiedei
Energy optimal design of servo-actuated systems: a concurrent approach based on scaling rules
Renewable and Sustainable Energy Reviews, Volume 156, March 2022, 111923
https://doi.org/10.1016/j.rser.2021.111923

above the traditionally suggested unitary value.

References

[1] Shyi-Min Lu. A review of high-efficiency motors: Specification, policy, and technology. Renewable and Sustainable Energy Reviews, 59:1–12, 2016.

[2] A De Almeida, J Fong, CU Brunner, R Werle, and M Van Werkhoven. New technology trends and policy needs in energy efficient motor systems - a major opportunity for energy and carbon savings. Renewable and Sustainable Energy Reviews, 115:109384, 2019.

[3] Rahman Saidur. A review on electrical motors energy use and energy savings. Renewable and Sustainable Energy Reviews, 14(3):877–898, 2010.

[4] Marek Lukaszczyk. Improving efficiency in electric motors. World Pumps, 4:34–41, 2014.

[5] Giovanni Carabin, Erich Wehrle, and Renato Vidoni. A review on energy-saving optimization methods for robotic and automatic systems. Robotics, 6(4):39, 2017.

[6] Alberto Richiedei, Dario; Trevisani. Optimization of the energy consumption through spring balancing of servo-actuated mechanisms. Journal of Mechanical Design, 142:012301 (10 pages), 2020.

[7] Roberto Belotti, Dario Richiedei, Iacopo Tamellin, and Alberto Trevisani. Response optimization of underactuated vibration generators through dynamic structural modification and shaping of the excitation forces. The International Journal of Advanced Manufacturing Technology, 112(1):505–524, 2021.

[8] Dario Richiedei and Alberto Trevisani. Analytical computation of the energy-efficient optimal planning in rest-to-rest motion of constant inertia systems. Mechatronics, 39:147–159, 2016.

[9] Andrea Trianni, Enrico Cagno, and Davide Accordini. Energy efficiency measures in electric motors systems: A novel classification highlighting specific implications in their adoption. Applied Energy, 252:113481, 2019.

[10] Anibal TI Ferreira, Fernando JTE; De Almeida. Induction motor downsizing as a low-cost strategy to save energy. Journal of Cleaner Production, 24:117–131, 2012.

[11] WITTENSTEIN alpha. Alpha advanced line datasheet. `https://alpha.wittenstein.de/en-en/products/alpha-advanced-line/`, 2020.

[12] K.A. Pasch and W.P. Seering. On the drive systems for high-performance machines. Journal of Mechanisms, Transmissions, and Automation in Design, 106(1):102–108, 1984.

This is a pre-print of the article: P. Boscariol, D. Richiedei
Energy optimal design of servo-actuated systems: a concurrent approach based on scaling rules
Renewable and Sustainable Energy Reviews, Volume 156, March 2022, 111923
https://doi.org/10.1016/j.rser.2021.111923

[13] Gill Hurley. Energy management of a servo motor - effects of inertia ratio. White paper, published online on https://www.kollmorgen.com/en-us/service-and-support/knowledge-center/white-papers/energy-management-of-a-servo-motor-effects-of-inertia-ratio/, 2015.

[14] Herman J Van de Straete, Pascal Degezelle, Joris De Schutter, and Ronnie JM Belmans. Servo motor selection criterion for mechatronic applications. IEEE/ASME Transactions on mechatronics, 3(1):43–50, 1998.

[15] Giancarlo Cusimano. A procedure for a suitable selection of laws of motion and electric drive systems under inertial loads. Mechanism and machine theory, 38(6):519–533, 2003.

[16] Giancarlo Cusimano. Generalization of a method for the selection of drive systems and transmissions under dynamic loads. Mechanism and machine theory, 40(5):530–558, 2005.

[17] Fredrik Roos, Hans Johansson, and Jan Wikander. Optimal selection of motor and gearhead in mechatronic applications. Mechatronics, 16(1):63–72, 2006.

[18] Erick A Padilla-Garcia, Alejandro Rodriguez-Angeles, Juvenal R Resendiz, and Carlos A Cruz-Villar. Concurrent optimization for selection and control of AC servomotors on the powertrain of industrial robots. IEEE Access, 6:27923–27938, 2018.

[19] Francesco Meoni and Marco Carricato. Optimal selection of the motor-reducer unit in servo-controlled machinery: A continuous approach. Mechatronics, 56:132–145, 2018.

[20] Dario Richiedei. Integrated selection of gearbox, gear ratio, and motor through scaling rules. Mechanics based design of Structures and Machines, 46(6):712–729, 2018.

[21] Marc Budinger, Jonathan Liscouët, F Hospital, and JC Maré. Estimation models for the preliminary design of electromechanical actuators. Proceedings of the Institution of Mechanical Engineers, Part G: Journal of Aerospace Engineering, 226(3):243–259, 2012.

[22] Pragasan Pillay and Ramu Krishnan. Modeling of permanent magnet motor drives. IEEE Transactions on industrial electronics, 35(4):537–541, 1988.

[23] Christian Hansen, Julian Öltjen, Davis Meike, and Tobias Ortmaier. Enhanced approach for energy-efficient trajectory generation of industrial robots. In 2012 IEEE International Conference on Automation Science and Engineering (CASE), pages 1–7. IEEE, 2012.

This is a pre-print of the article: P. Boscariol, D. Richiedei
Energy optimal design of servo-actuated systems: a concurrent approach based on scaling rules
Renewable and Sustainable Energy Reviews, Volume 156, March 2022, 111923
https://doi.org/10.1016/j.rser.2021.111923

[24] Ilaria Palomba, Erich Wehrle, Giovanni Carabin, and Renato Vidoni. Minimization of the energy consumption in industrial robots through regenerative drives and optimally designed compliant elements. Applied Sciences, 10(21):7475, 2020.

[25] G Carabin, L Scalera, T Wongratanaphisan, and R Vidoni. An energy-efficient approach for 3D printing with a linear delta robot equipped with optimal springs. Robotics and Computer-Integrated Manufacturing, 67:102045, 2021.

[26] Kaoru Inoue, Yuji Asano, Keito Kotera, and Toshiji Kato. Optimal energy saving trajectories of induction motor with suppression of sudden acceleration and deceleration. In 2014 IEEE Energy Conversion Congress and Exposition (ECCE), pages 3219–3223. IEEE, 2014.

[27] Hakan Gurocak. Industrial motion control: motor selection, drives, controller tuning, applications. John Wiley & Sons, 2015.

[28] John H Evans. Dimensional analysis and the Buckingham π theorem. American Journal of Physics, 40(12):1815–1822, 1972.

[29] Tatjana Misic, Marina Najdanovic-Lukic, and Ljubisa Nesic. Dimensional analysis in physics and the Buckingham theorem. European Journal of Physics, 31(4):893, 2010.

[30] Kenneth J Waldron and Christopher Hubert. Scaling of robotic mechanisms. In Proceedings 2000 ICRA. Millennium Conference. IEEE International Conference on Robotics and Automation. Symposia Proceedings (Cat. No. 00CH37065), volume 1, pages 40–45. IEEE, 2000.

[31] Elias Saerens, Stein Crispel, Pablo López García, Tom Verstraten, Vincent Ducastel, Bram Vanderborght, and Dirk Lefeber. Scaling laws for robotic transmissions. Mechanism and Machine Theory, 140:601–621, 2019.

[32] Giuseppe Ricci. Weight and rated characteristics of machines: positive displacement pumps, motors and gear sets. Mechanism and machine Theory, 18(1):1–6, 1983.

[33] Y. Duan and D. M. Ionel. Nonlinear scaling rules for brushless pm synchronous machines based on optimal design studies for a wide range of power ratings. IEEE Transactions on Industry Applications, 50(2):1044–1052, 2014.

[34] Giuseppe Ricci. Mass and rated characteristics of planetary gear reduction units. Meccanica, 27(1):35–45, 1992.

[35] Marc Budinger, Aurélien Reysset, Aitor Ochotorena, and Scott Delbecq. Scaling laws and similarity models for the preliminary design of multirotor drones. Aerospace Science and Technology, 98:105658, 2020.

This is a pre-print of the article: P. Boscariol, D. Richiedei
Energy optimal design of servo-actuated systems: a concurrent approach based on scaling rules
Renewable and Sustainable Energy Reviews, Volume 156, March 2022, 111923
https://doi.org/10.1016/j.rser.2021.111923

[36] Joachim Kurzke and Claus Riegler. A new compressor map scaling procedure for preliminary conceptional design of gas turbines. In Turbo Expo: Power for Land, Sea, and Air, volume 78545, page V001T01A006. American Society of Mechanical Engineers, 2000.

[37] Marc Budinger, Jonathan Liscouët, Yu Cong, and Jean-Charles Maré. Simulation based design of electromechanical actuators with Modelica. In International Design Engineering Technical Conferences and Computers and Information in Engineering Conference, volume 49002, pages 231–240, 2009.

[38] Sangok Seok, Albert Wang, David Otten, and Sangbae Kim. Actuator design for high force proprioceptive control in fast legged locomotion. In 2012 IEEE/RSJ International Conference on Intelligent Robots and Systems, pages 1970–1975. IEEE, 2012.

[39] Juha Saari et al. Thermal analysis of high-speed induction machines. Helsinki University of Technology, 1998.

[40] Luc Houpert. Ball bearing and tapered roller bearing torque: analytical, numerical and experimental results. Tribology transactions, 45(3):345–353, 2002.

[41] Jafar Takabi and MM Khonsari. Experimental testing and thermal analysis of ball bearings. Tribology international, 60:93–103, 2013.

[42] Tomasz Piatkowski. Dahl and LuGre dynamic friction models-the analysis of selected properties. Mechanism and Machine Theory, 73:91–100, 2014.

[43] Pedro Andrada Gascón, Marcel Torrent Burgués, Josep Ignasi Perat Benavides, and Balduino Blanqué Molina. Power losses in outside-spin brushess dc motor. Renewable Energy and Power Quality Journal, 2:320–1, 2004.

[44] Giovanni Legnani, Riccardo Adamini, Monica Tiboni, and Diego Tosi. Meccanica degli Azionamenti. Azionamenti Elettrici: Principi di funzionamento, accoppiamento con il carico, scelta del gruppo motore-riduttore, leggi di moto, controllo. Società Editrice Esculapio, 2016.

[45] Joseph Edward Shigley. Shigley's mechanical engineering design. Tata McGraw-Hill Education, 2011.

[46] Roberto Caracciolo and Dario Richiedei. Optimal design of ball-screw driven servomechanisms through an integrated mechatronic approach. Mechatronics, 24(7):819–832, 2014.

[47] RW America. BKL series copulings datasheet. `https://www.rw-america.com/products/precision-couplings/metal-bellows-couplings/bkl/`, May 2020.

This is a pre-print of the article: P. Boscariol, D. Richiedei
Energy optimal design of servo-actuated systems: a concurrent approach based on scaling rules
Renewable and Sustainable Energy Reviews, Volume 156, March 2022, 111923
https://doi.org/10.1016/j.rser.2021.111923

[48] Osama Al-Naseem, Robert W Erickson, and Palmer Carlin. Prediction of switching loss variations by averaged switch modeling. In APEC 2000. Fifteenth Annual IEEE Applied Power Electronics Conference and Exposition (Cat. No. 00CH37058), volume 1, pages 242–248. IEEE, 2000.

[49] Ahmed Abdelhakim, Frede Blaabjerg, and Paolo Mattavelli. Modulation schemes of the three-phase impedance source inverters - part ii: Comparative assessment. IEEE Transactions on Industrial Electronics, 65(8):6321–6332, 2018.

[50] Kollmorgen. Kollmorgen automation solutions and product catalog emea. published online on `https://www.kollmorgen.com/en-us/products/catalogs/kollmorgen-automation-solutions-catalog-emea/`, 2018.

This is a pre-print of the article: P. Boscariol, D. Richiedei
Energy optimal design of servo-actuated systems: a concurrent approach based on scaling rules
Renewable and Sustainable Energy Reviews, Volume 156, March 2022, 111923
https://doi.org/10.1016/j.rser.2021.111923